Direct estimation of sea state impacts on radar altimeter sea level measurements

D. Vandemark

NASA/Goddard Space Flight Center, Wallops Island, Virginia

N. Tran[1], B. D. Beckley

Raytheon/ITSS, Greenbelt, Maryland

B. Chapron

IFREMER/Centre de Brest, Plouzané, France

P. Gaspar

Collecte Localisation Satellites, Ramonville, France

Short title: DIRECT SEA STATE BIAS ESTIMATION

Abstract.

Uncertainty remains in sea state bias (SSB) range correction models used to aid precision sea level estimation by satellite altimeters. The models are typically developed empirically, using an indirect, satellite range measurement differencing approach that has several limitations. A more direct SSB estimation technique is examined here. It takes advantage of the long-term TOPEX/Poseidon precision altimetry mission, a mission that envelops error reduction in every facet of the altimeter's error budget. It is shown that the TOPEX SSB, resolved using direct analysis of the global sea surface height residuals uncorrected for sea state driven range biases, agrees closely with the most current nonparametric SSB model. Besides a new found validation source for difference-based TOPEX and JASON-1 altimeter models, this alternative should greatly ease the study of unresolved basin-scale SSB variation and the examination of SSB residual error associated with long wave properties not measured by the altimeter.

Introduction

The model for an altimeter's sea state bias (SSB) remains one of the more uncertain terms in precision ocean altimetry. Range uncertainty is thought to be 1.5-2 cm on average and can exceed 5 cm in high seas [*Chelton et al.,* 2001]. The SSB is largely due to the electromagnetic bias observation that wave surface nonlinearities act to reflect normally incident radiation more strongly, per unit square area, from wave troughs than from the crests [*Yaplee et al.,* 1971]. Satellite altimeters carry this EM bias within a total SSB that can also include satellite-specific sea state range error dependencies.

The SSB range correction algorithm used by a given satellite is determined empirically by making use of an observed relationship between range error and two additional radar altimeter products, the radar cross section and significant wave height (SWH). Methods for deriving this model using satellite data have, to date, required an indirect method to acquire the SSB range error term due to large uncertainties in orbit and/or geoid height estimates that overwhelm any attempt to observe the SSB directly in residual sea surface height data (for review, see Chelton et al. [2001]). For TOPEX/Poseidon the orbit errors are minimal, but the geoid must still be removed. A location's sea surface height measurement uncorrected for SSB, SSH, contains the geoid signal (h_g), the ocean dynamic topography (η), the SSB, and other measurement and correction noise sources (w):

$$SSH' = h_g + \eta' + SSB' + w'. \tag{1}$$

The apostrophe denotes time-dependent factors. To resolve the small SSB range signal,

the dominant marine geoid signal is eliminated from this equation by differencing precise repeat measurements either along collinear tracks [*Chelton,* 1994] or at crossover points [*Gaspar et al.,* 1994]. The altimeter repeat measurements typically occur within 3-17 days for TOPEX or Geosat, thus longer-term variance in the large η term is also removed. SSB estimation must then relate a time-dependent range difference, $\Delta h'$, to corresponding wave height and wind speed differences.

While relatively successful, the development of SSB models based on repeat-pass differences rather than the direct correlatives presents several limitations as discussed in Gaspar et al. [2001]. Key among these is the need to develop a nonparametric model function to resolve nonlinearities obscurred within standard regression techniques operating on differenced data. In addition, it is not possible to perform residual error analysis. Large amounts of data and complex, numerically-optimized computations are also required to properly develop such a model. Finally, solution complexity limits flexibility in dealing with tests of new ancillary variables, such as global wave products, that may lead to improvements in this range correction.

Another approach is to solve for SSB directly by imposing a constant *a priori* mean sea level for each altimeter observation location, thus eliminating the geoid. This method was rejected in past studies due to noise in developing such reference. But the TOPEX/Poseidon mission has now provided 10 years of precision measurements along the same 254 ground tracks across the global ocean. The TOPEX/Poseidon georeferenced altimeter surface height dataset compilation [*Koblinsky et al.,* 1998] provides much of the data needed to revisit this direct inversion of Eq. 1, including

the necessary mean surface reference data set along the TOPEX ground track [*Wang,* 2001]. Hereafter, we describe the method, data and results of direct SSB solution as found by relating surface height residuals to altimeter SWH and wind speed parameters. Comparisons, implications and limitations of the new approach are discussed.

Methods

Following Eq. 1, a long-term average for the sea surface (MSS) at any referenced location, k, on an altimeter's ground track can be written as:

$$MSS_k = h_{g,k} + < \eta' >_k + < SSB' - SSB'_m >_k + < w' >_k \quad (2)$$

where <> denotes the local long-term average (or local expectation, as used in the process of MSS estimation). SSB_m are the model-estimated sea state range corrections employed in this surface determination, and w comprises all other error components (e.g. in sensor range corrections, interpolation errors, orbit, tides, atmospheric terms, etc...) built into the MSS estimate. Time dependence is denoted to highlight averaging effects to be discussed later. Eq 2. is written assuming independence between source terms and MSS_k is largely defined by the marine geoid and the averaged ocean dynamic topography at location k.

An individual height residual, $\Delta h'_k$, used in SSB estimation is thus:

$$\Delta h'_k = (SSH'_k - MSS_k) = SSB'_k + (\eta' - < \eta >)_k - \epsilon_{SSB,k} + (w' - < w >)_k \quad (3)$$

where $\epsilon_{SSB,k} =< SSB - SSB_m >$ is now the time-independent SSB modeling error derived for each MSS_k estimate. The apostrophe is dropped within the expectations

to differentiate the realizations that form MSS_k from the arbitrary samples denoted in Eq. 4. Next, dynamic sea level variability $(\eta' - <\eta>)_k$ is joined with $(w' - <w>)_k$ to form a noise term ϵ_k that is assumed independent from sea state effects to first-order. The geoid term has also dropped from Eq. 3 to give:

$$\Delta h'_k = SSB(U', SWH')_k + \epsilon_{SSB,k} + \epsilon_k. \tag{4}$$

where explicit SSB dependence on radar cross section derived wind speed, U, and SWH is assigned. Error terms on the right side of the equation depend critically upon the quality of the estimates that go into the time series average used to build MSS_k, while ϵ_{SSB} is also related to the accuracy of the SSB model estimates used.

A globally-derived SSB estimate can be built by defining MSS_k on a global scale and then computing the mean sea state bias for discrete bins in the two-dimensional (U, SWH) domain. These expectations are computed over height residuals at any location, k_{ij}, meeting the condition that altimeter derived wind and wave height estimates fall within a (U_i, SWH_j) bin having width $(\Delta U, \Delta SWH)$, given as:

$$SSB(U_i, SWH_j) = < SSH'_{k,ij} - MSS_{k,ij} > \tag{5}$$

The ϵ terms are dropped from Eq. 4 following the assumptions of independence from sea state effects and the convergence of $<\eta'>$ and $<w'>$ towards zero mean values under long-term global averaging. These assumptions are addressed in following sections.

Implementation of this formulation using TOPEX NASA altimeter (TOPEX hereafter) data is straightforward. The sea surface height residuals, $\Delta h'$, used are interpolated, georeferenced values computed along the TOPEX track using the reference

mean sea surface (MSS), GSFC00 [*Wang,* 2001]. This surface merges multiple years of several satellite altimeter mission data (TOPEX, ERS, and Geosat) along the mean tracks of TOPEX (see the NASA Ocean Altimeter Pathfinder Project [*Koblinsky et al.,* 1998]), spanning a time period from 1986 to 1999. The large time period and number of repeat measurements lead to a precise geoid determination along the TOPEX track. This provides not only a reference mean sea level for oceanic studies, but also a low noise MSS along the altimeter's ground track that was not available in past SSB investigations.

Prior to computing $\Delta h'$, TOPEX sea surface heights are corrected for all geophysical and instrumental effects. Since standard environmental corrections (wet and dry tropospheric, ionospheric, inverse barometer, ocean tide, solid Earth tide, load tide, and pole tide corrections, including the sea state bias correction) were applied to each TOPEX sea level estimate, the original sea state bias correction (version 2.0 algorithm [*Gaspar et al.,* 1994]) is removed from each residual estimate. These estimates are given at 1-second along-track intervals ($\sim$ every 6 km), interpolated to fixed georeferenced track locations. A quality control file that contains a flagword for each observation is also provided in the dataset. All Poseidon-1 altimeter and any flagged TOPEX estimates are eliminated from the study.

Pairing of the NASA/GSFC Altimeter Pathfinder dataset with both Ku-band normalized radar cross-section (σ_0) and SWH data is accomplished using the same georeferencing interpolation. Altimeter wind speed is the 10-m wind speed calculated from σ_0 using the modified Chelton and Wentz algorithm [*Witter and Chelton,* 1991].

Anomalous height data within any (U, SWH) bin are flagged and removed if the height residual lies outside of ± 5 standard deviations from the mean. One 10-day TOPEX cycle of pathfinder data prepared in this manner provides 350,000-400,000 data points for SSB study. For this work, cycles 21-131, April 1993-April 1996, are examined. Total samples used in a 3-year average exceeds forty million realizations. For demonstrations here, the data are not spatially subsampled to assure independence, but such sampling to a 70-100 km along track grid spacing would reduce the number of samples used by a factor of about ten. By comparison, the same period's crossover data set [*Gaspar et al.,* 2001] yields 633,000 samples.

Results

The method discussed above is the most simplistic, direct approach to resolve sea state bias effects using on-orbit data, but numerous assumptions must be met to achieve success. Two immediate questions arise: what is the validity of the assumption that ϵ_k is a zero-mean random error term and how does one evaluate the magnitude of $< \epsilon_{SSB}(U_i, SWH_j) >$ and its impact on direct SSB inversion?

To address the first question, sample global $< \Delta h' >$ data for U = 7.75 m/s and SWH = 2.0 m (± 0.125 m/s, 0.125 m) is given in Fig. 1, as collected from 1993-1996. The sea state bias of 7 cm is apparent. Scatter indicates a substantial 8 cm standard deviation, but also that the distribution has a quasi-Gaussian shape allowing assumption that ϵ_k behaves as a random error term. This is in accord with the central limit theorem and suggests the Pathfinder residual SSH dataset is eligible for our purpose. Recall that

this expectation is carried out over a global sampling and for three years where one can anticipate that $< \eta' >_{k,ij}$ would tend to a near-zero value.

The second question is less directly answered. In the ideal case, where all the (U, SWH) related variability has been retrieved by the SSB model used for the MSS_k determinations, ϵ_{SSB} is uncorrelated with (U, SWH) and consequently $< \epsilon_{SSB} > \equiv constant$. Little difference between this method and the crossover approach is thus expected. Note that assignment to a small cm-level constant here, rather than 0.0, is a feature of the unknown absolute reference in SSB_m that is common to differenced SSB models [e.g. [*Gaspar et al.,* 1994]]. On the other hand, if somewhat imperfect SSB models have been used (most likely the case, especially for Geosat and ERS) one can expect that correlation remains between (U, SWH) and $< \epsilon_{SSB} >_k$. This possibility is reduced however by averaging used to develop MSS_k. Different sensors, and hence SSB models, and many different (SSH', U_i, SWH_j) realizations are included in the estimation of each mean surface value. One can expect that these factors act to reduce $< \epsilon_{SSB} >_k$ to a small nearly constant value over much of the (U, SWH) domain. Under these assumptions, Eq. 5 becomes:

$$< SSH'(U_i, SWH_j)_k - MSS_k > \approx SSB(U_i, SWH_j) + constant \qquad (6)$$

Overall direct SSB results are now compared with the Gaspar et al. [2001] crossover model (hereafter denoted NP01) obtained for the same TOPEX period, cycles 21-131. Fig. 2 shows the bin-averaged residual SSH data in the (U, SWH) domain with a bin width of 0.25 m/s in U and 0.25 m in SWH. Each bin contains at least 200 data points

or it is not presented. The extent of the domain is shown by the shaded area and corresponds to this dense data region. Contours are provided to visualize the features. Note that this is the first reported direct (non-differenced) realization of on-orbit sea state bias impacts. Moreover, the results are directly in a tabular form that mimics the current NP model output format. While not shown, the crossover-based NP01 model solution looks nearly identical to Fig. 2.

As mentioned, a limitation encountered in this or the crossover method comes in resolving the absolute model reference to better than a small cm-level uncertainty. For the crossover approach, only SSB differences are observed so that the SSB can only be determined to within a constant. To eliminate this undetermination one must impose a somewhat arbitrary value for the SSB. One obvious choice is to set the SSB to zero over a flat sea with no wind, i.e. $SSB(0,0) = 0$. However, since the data density close to (0,0) is sparse; this solution is not considered. This crossover method uses a first guess value for the bias at a position near the median in the joint (U, SWH) distribution, to determine a SSB solution, and then shifts the solution at all grid points to satisfy $SSB(0,0) = 0$.

In the present approach, a bias is also observed, likely due to the term $< \epsilon_{SSB} >$ that is assumed to have a nearly constant value over the (U, SWH) domain.

Due to these issues in absolute reference, a level shift between the directly-obtained residual map (Fig. 2) and the NP01 model solution is not unexpected. Direct comparison between results is obtained after adjusting the present SSB estimates to match NP01 at the point U = 7.75 m/s and SWH = 2.0 m, the median bin. The shift

used is 1.6 cm and has been applied in the results shown in Fig. 2. Possible use of other points within the dense data zone indicates that shift values vary by only a few mm. This ΔSSB shift between the two results yields respectively 1.4 cm for the bin (5.75 m/s, 1.75 m) and 2.0 cm for data centered at (9.25 m/s, 2.5 m).

Direct comparison with the NP01 model grid is given in Fig. 3. Results of Fig. 3(a) represents the difference between methods. It is found that 86% of the bin-averaged SSB estimates differ by less than 1.0 cm and 57% by less than 0.5 cm. This high level of agreement is exceptional and helps to corroborate this recent NP01 model. At the same time, agreement tends to validate the use of this alternate approach to estimate SSB, confirming that ϵ_{SSB} could be assumed, to first-order, uncorrelated with (U, SWH). The far edges of the comparison domain do exhibit some higher values and these differences are yet to be explored. For example, no spatial equalization within the global averaging has been performed. Such optimization could act to further refine the raw estimates shown here.

One potential advantage to the present method is the ability to develop an SSB model using less data gathered over a shorter period of time. This capability could benefit development of SSB models for TOPEX follow-on altimeters such as Jason-1 and -2. To examine how much data is necessary, the time period for TOPEX averaging is reduced to 1 year. Fig. 3(b) shows a 1-year (cycles 21-57) SSB difference map, the agreement is comparable to the 3-year differences with 84% of the bins with ΔSSB under 1.0 cm and 54% under 0.5 cm. Results for two other 1-year periods, cycles 57-94 and 94-131, show similar results. In assessing these differences, different values for

the absolute shift were applied with respect to the time frame. These are respectively 1.7, 1.3, and 1.8 cm for the three successive 1-year periods. Fig. 3(c) shows the SSB differences obtained using an average over only 100 days, cycles 75-85, have 77% of the bins showing ΔSSB under 1.0 cm and 49% under 0.5 cm. Again, the largest ΔSSB occur at the limits of the dense data region. The level shift in this case is 1.3 cm. Agreement between the 3-year NP01 map and the 10-cycle one is remarkable, given the brute force technique applied here. Analyses of other 10-cycle error maps exhibit similar variation over the limits of the domain. This suggests that there is enough data collected within 100 days to develop a reasonable first estimate of the SSB mapping in the densest data zone in the (U, SWH) domain while a 1-year period would provide a global mapping.

The variation in the absolute shift values applied above is small, in the mm range, but still of some concern in context of corrections applied within precision altimetry. Reflection on the origin of this variance suggests at least three potential time-dependent sources: $< \epsilon_{SSB} = f(U(t), SWH(t)) >$ as discussed earlier; uncertainty in the reference level related to its time dependence that can be separated in two sources - deterministic dynamic topography variation and mean sea level rise.

Indeed, the chosen reference surface, MSS, is a combination of marine geoid and the ocean dynamic topography computed over many years and using multiple satellite altimeter mission data, specifically to remove this same dynamic topographic signal that dominates the $\Delta h'$ used in the present study. Fig. 4 shows this cycle-by-cycle ($< SSH' - MSS_k >$) estimates versus time as collected in the bin (U = 7.75 m/s, SWH

= 2.0 m). Annual and semi-annual harmonics present in the residual data are unrelated to the SSB, and show interannual surface variability correlated with global-average sea surface temperature variations [*Nerem,* 1995; *Minster et al.,* 1995]. Moreover superimposed upon this variability is a longer-term mean sea level variation. Nerem and Mitchum [2001] report that the rate of change of global mean sea level derived from 6 years of TOPEX/Poseidon data, 1993-1998, is +2.5 mm/year. Thus both the global dynamic topography and the mean sea level rise may affect results in terms of absolute, but not relative, bias versus time. It is anticipated that these factors may be addressed by further space/time optimization (e.g. filtering, equalization) during the bin-averaging process.

Conclusion

The sea state bias impact on altimeter range estimates is presented based on a simple bin-averaging procedure using global TOPEX sea surface height residuals. Data come from the georeferenced NASA/GSFC altimeter pathfinder database. The original sea state bias correction is removed from each height estimate and the residual is then computed with respect to a reference mean sea surface (MSS), GSFC00 [*Wang,* 2001] , that carries high precision along the TOPEX ground tracks. Results from a 3-year global average mirror that obtained using satellite crossover differences and subsequent nonparametric model inversion. This validation via intercomparison corroborates two separate empirical realizations of the TOPEX sea state bias, but it is recognized that the alternative method presented above requires optimization before its full potential

can be assessed.

There is no question that this direct method is a much simpler technique to implement from numerous perspectives, most clearly the removal of any need for complex and numerically-intensive nonparametric inversion. Moreover, one is now working directly with the residual and its correlatives, rather than time-dependent differences in each term. These points together suggest the benefit that such direct assessment may have in speeding studies to refine physical insight and empirical models for this sea state effect. For example, direct regression of TOPEX height residuals against global model-derived long wave products, unobtainable using the altimeter, are in progress. It is also shown here that an empirical SSB estimate over most of the (U, SWH) domain can be obtained with as little as 100 days of data. This same sparse sampling approach can be applied spatially, where basin-scale evaluation of the sea state impacts now becomes more tractable.

Limitations of this approach start with the reliance upon the long-term TOPEX repeat track mission. This precision altimetry program provides a highly accurate mean sea surface reference at every point along the global ocean ground track, but also optimized corrections for many components (e.g. tides, orbit, ionosphere, water vapor, sensor,...) that are applied to the individual TOPEX/Poseidon (and its follow on Jason-1) range measurements. Thus, it is postulated that the same methodology may not apply to altimeters aboard ERS, Envisat, or Geosat Follow-On platforms. As importantly, this method relies on random processes within the observed residual that converge to a zero mean and that are independent, to first-order, from the altimeter

radar cross section and wave height parameters. While these assumptions appear to hold at the cm level, future work will attempt to correct for observed mm-level variance in absolute bias ascribed to seasonal and interannual variability in the dynamic topography.

References

Chelton D.B.: The sea state bias in altimeter estimates of sea level from collinear analysis of TOPEX data, *J. Geophys. Res.*, 99, 24995-25008, 1994.

Chelton, D. B., Ries, J. C., Haines, B. J., Fu L.-L., and P. S. Callahan, Satellite altimetry, in Satellite Altimetry and Earth Sciences, Ed. Fu L. and Cazenave A. , *Int. Geophys. Series*, 69, 1-131, 2001.

Gaspar P. and J.P. Florens: Estimation of the sea state bias in radar altimeter measurements of sea level: Results from a new nonparametric method, *J. Geophys. Res.*, 103, 15803-15814, 1998.

Gaspar P., S. Labroue, F. Ogor, G. Lafitte, L. Marchal, and M. Rafanel: Improving nonparametric estimates of the sea state bias in radar altimeter measurements of sea level, submitted to *J. Atmos. Oceanic Technol.*, 2001.

Gaspar P., F. Ogor, P.-Y. Le Traon, and O.-Z. Zanife: Estimating the sea state bias of the TOPEX and POSEIDON altimeters from crossover differences, *J. Geophys. Res.*, 99, 24981-24994, 1994.

Koblinsky C.J., B.D. Beckley, R.D. Ray, Y.M. Wang, L. Tsaoussi, A. Brenner, and R. Williamson, NASA Ocean Altimeter Project, Report 1, in Data Processing Handbook, NASA Tech. Memo, TM-1998-208605, 1-43, 1998.

Minster J.-F., C. Brossier, and P. Rogel: Variation of the mean sea level from TOPEX/POSEIDON data, *J. Geophys. Res.*, 100, 25153-25161, 1995.

Nerem R.S.: Measuring global mean sea level variations using TOPEX/POSEIDON altimeter data, *J. Geophys. Res.*, 100, 25135-25151, 1995.

Nerem R.S. and G.T. Mitchum: Sea level change, in Satellite altimetry and Earth sciences, Ed. Fu. L. and Cazenave A., *Intl. Geophys. Series*, 69, 329-347, 2001.

Wang Y.M.: GSFC00 mean sea surface, gravity anomaly, and vertical gravity gradient from satellite altimeter data, J. Geophys. Res., 106, 31167-31174, 2001.

Yaplee, B.S., A. Shapiro, D.L. Hammond, B.D. Au and E.A. Uliana, Nanosecond radar observations of the ocean surface from a stable platform, *IEEE*, GE-9, 170-174 , 1971.

Witter D.L. and D.B. Chelton: A GEOSAT wind speed algorithm and a method for altimeter wind speed development, J. Geophys. Res., 96, 8853-8860, 1991.

D. Vandemark, OPAL, University of New Hampshire, Rm. 142 Morse, Durham, NH 03824 (email: vandemark@gsfc.nasa.gov).

Received June 01, 2002

---

[1]Now at CLS, Ramonville, France.

Figure 1. Histogram of TOPEX residual SSH observations at 7.75 ± 0.125 m/s in U and 2.0 ± 0.125 m in SWH. Statistics, including number of samples, are noted, and a Gaussian function carrying the same variance is shown.

Figure 2. Isolines for the global SSB estimate (in meters) obtained from bin-averaging of the data in boxes of width (0.25 m/s, 0.25 m) over the (U, SWH) domain. All SSB values are shifted upward 1.6 cm. The shaded area corresponds to boxes containing at least 200 measurements during the 3-year subset, TOPEX cycles 21-131.

Figure 3. Difference between the shifted bin-averaged map and the Gaspar et al. [2001] model grid (in meters). The bin-averaged estimate were computed by using (a) a 3-year subset, cycles 21-131; (b) a 1-year subset, cycles 21-57; and (c) a 10-cycle subset, cycles 75-85.

Figure 4. 1-cycle estimates of $(< SSH'_k - MSS_k >)$ in the bin centered at (7.75 m/s, 2.0 m) and a smoothing curve using a 3-cycle averaging window.

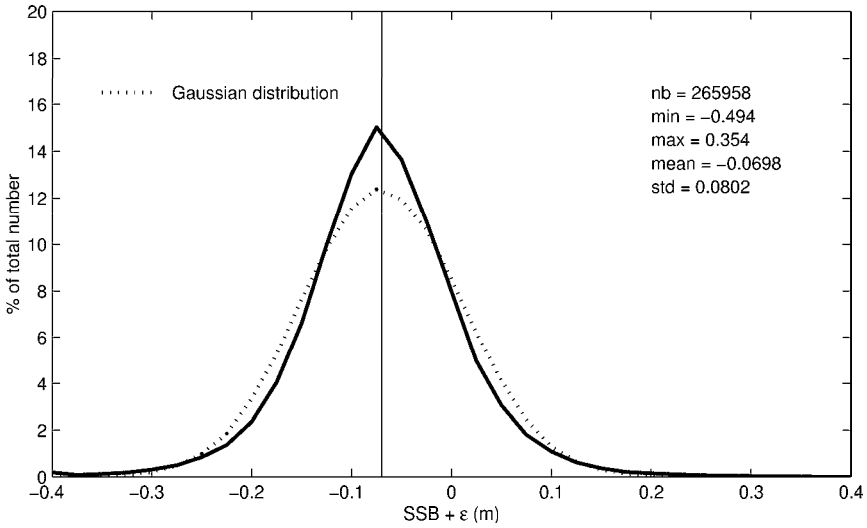

Figure 1. Histogram of TOPEX residual SSH observations at 7.75 ± 0.125 m/s in U and 2.0 ± 0.125 m in SWH. Statistics, including number of samples, are noted, and a Gaussian function carrying the same variance is shown.

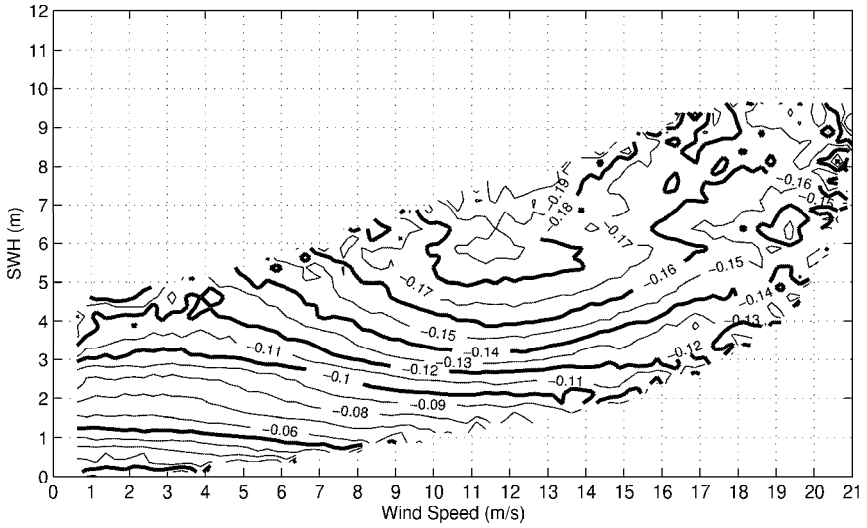

Figure 2. Isolines for the global SSB estimate (in meters) obtained from bin-averaging of the data in boxes of width (0.25 m/s, 0.25 m) over the (U, SWH) domain. All SSB values are shifted upward 1.6 cm. The shaded area corresponds to boxes containing at least 200 measurements during the 3-year subset, TOPEX cycles 21-131.

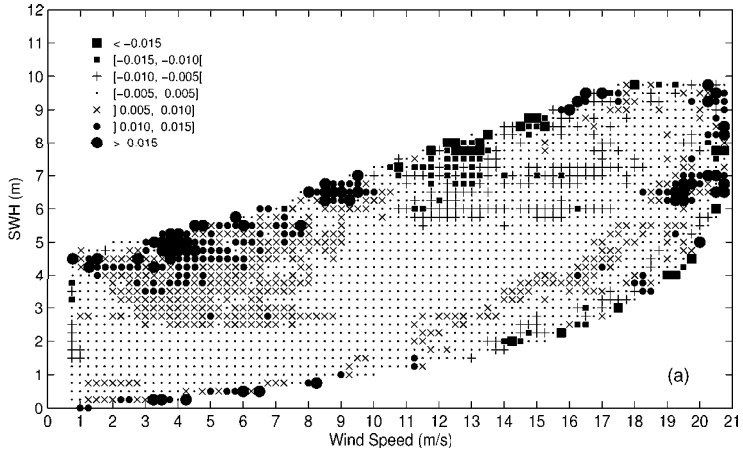
< −0.015
[−0.015, −0.010[
[−0.010, −0.005[
[−0.005, 0.005]
] 0.005, 0.010]
] 0.010, 0.015]
> 0.015
SWH (m)
Wind Speed (m/s)
(a)

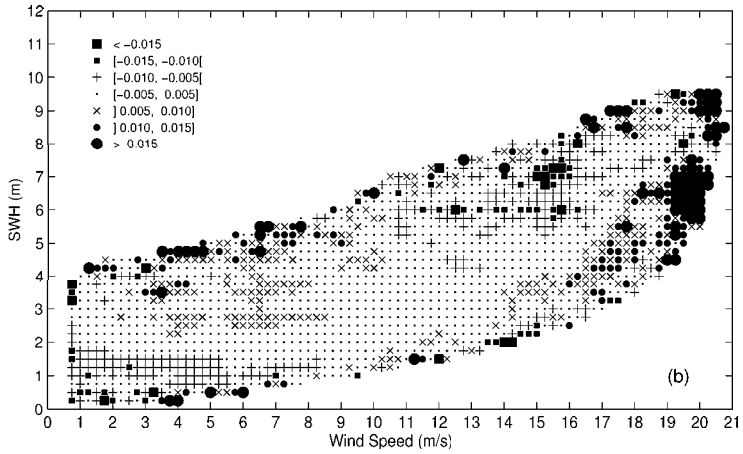
< −0.015
[−0.015, −0.010[
[−0.010, −0.005[
[−0.005, 0.005]
] 0.005, 0.010]
] 0.010, 0.015]
> 0.015
SWH (m)
Wind Speed (m/s)
(b)

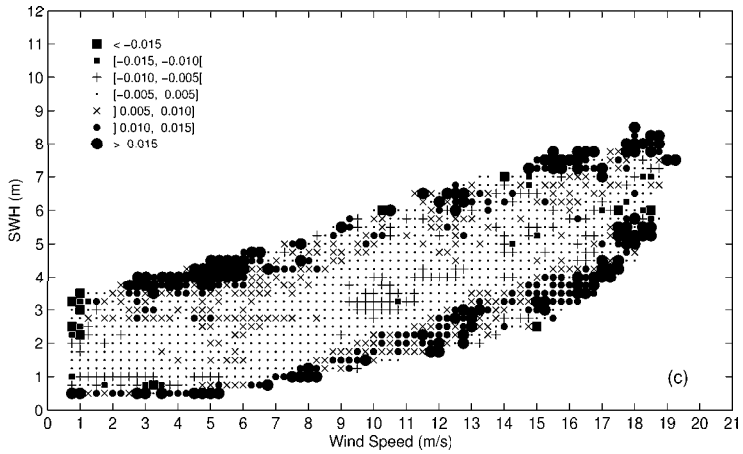
< −0.015
[−0.015, −0.010[
[−0.010, −0.005[
[−0.005, 0.005]
] 0.005, 0.010]
] 0.010, 0.015]
> 0.015
SWH (m)
Wind Speed (m/s)
(c)

Figure 3. Difference between the shifted bin-averaged map and the Gaspar et al. [2001] model grid (in meters). The bin-averaged estimate were computed by using (a) a 3-year subset, cycles 21-131; (b) a 1-year subset, cycles 21-57; and (c) a 10-cycle subset, cycles 75-85.

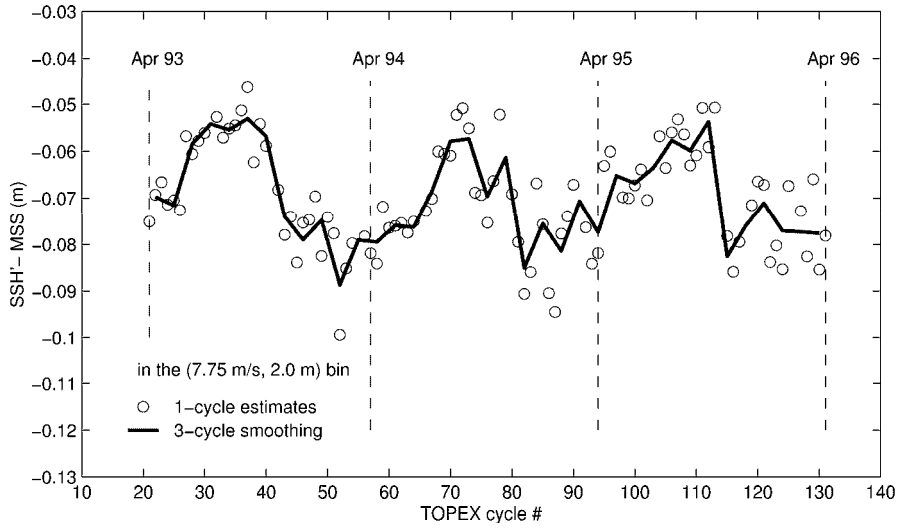

Figure 4. 1-cycle estimates of $(< SSH'_k - MSS_k >)$ in the bin centered at (7.75 m/s, 2.0 m) and a smoothing curve using a 3-cycle averaging window.